JOURNAL OF GUIDANCE, CONTROL, AND DYNAMICS
Vol. 29, No. 6, November–December 2006

Engineering Notes

ENGINEERING NOTES are short manuscripts describing new developments or important results of a preliminary nature. These Notes should not exceed 2500 words (where a figure or table counts as 200 words). Following informal review by the Editors, they may be published within a few months of the date of receipt. Style requirements are the same as for regular contributions (see inside back cover).

Aeroservoelastic Stability of Supersonic Slender-Body Flight Vehicles

Hassan Haddadpour*
Sharif University of Technology, 11365-8639 Tehran, Iran

DOI: 10.2514/1.13591

Introduction

THE coupling between flight mechanics, aeroelasticity, and control system is called aeroservoelasticity. Flight vehicles with slender configuration can experience aeroservoelastic instability during flight. This type of instability is likely to occur when short period rigid-body mode, body bending mode, and control loop mode are not properly phased. On the other hand, stable aeroservoelastic phenomena can affect the planned trajectory of the vehicle. For this reason the extent of aeroservoelastic interaction for guided supersonic vehicles is of considerable importance.

The dynamics of the elastic vehicles have been studied in various categories. Meirovitch and Nelson [1] examined the dynamic stability of a spin-stabilized spacecraft containing flexible rod appendages. Meirovitch and Wesley [2] presented an approach for nonspinning variable-mass rockets aeroelasticity whereas Oberholtzer et al. [3], Crimi [4], and Platus [5] investigated the same approach for spinning missiles. Whereas the researchers focused on special cases, an integrated approach developed for nonspinning elastic hypersonic flight vehicles by Bilimoria and Schmidt [6]. To predict the effect of body flexibility on control system Newman and Schmidt [7] developed a two-dimensional aeroelastic model of flight vehicles. The effect of flexibility on the poles and zeros of a general flexible flight vehicle has been studied by Livneh and Schmidt [8]. Thrust effect in the boost phase of flight on the vibrational characteristics of flexible guided vehicles has also been studied by Pourtakdoust and Assadian [9] numerically.

Using the previous works of Platus [5] and Bilimoria and Schmidt [6] on the aeroelasticity of unguided flight vehicles, the present work develops an analytical model for the study of aeroservoelasticity of guided supersonic slender body flight vehicles. For this purpose, modal analysis method is employed for the structure, slender body theory is used for aerodynamics, and rate-gyro and actuator dynamics in roll, pitch, and yaw channels are also considered in construction of the model. The solutions to the equations of motion are analyzed for instability prediction.

Received 22 September 2004; revision received 26 September 2005; accepted for publication 5 April 2005. Copyright © 2005 by Hassan Haddadpour. Published by the American Institute of Aeronautics and Astronautics, Inc., with permission. Copies of this paper may be made for personal or internal use, on condition that the copier pay the $10.00 per-copy fee to the Copyright Clearance Center, Inc., 222 Rosewood Drive, Danvers, MA 01923; include the code $10.00 in correspondence with the CCC.

*Assistant Professor, Department of Aerospace Engineering; haddadpour@sharif.edu.

Formulation

A flexible vehicle flying in space is illustrated in Fig. 1. Using the notation of Bilimoria and Schmidt [6], the inertial frame and body frame, which are defined in the standard fashion, are also shown in Fig. 1. The body frame is fixed to the body of the vehicle, with the origin at its center of mass. The elastic mean axes system is chosen as the body-axis system. The vehicle rotates in space with the angular velocity vector, $\boldsymbol{\omega}$, with the components p, q, and r about the body-fixed axes x, y, and z. The vehicle velocity vector ($\boldsymbol{V}$) components are denoted by u, v, and w with respect to the body-fixed frame of reference. Elastic deflections of the flexible vehicle are treated as the motion of particles relative to the body-fixed axes. Elastic motions are assumed to be a combination of bending deflections δy and δz in the y- and z-directions, respectively, and torsional rotation θ_x around the x-axis. On the other hand, the length of the body is assumed to be fixed so for small bending deflections along the y- and z-axes, the change along the x-axis is negligible.

For the derivation of the equations of motion, Lagrange's method is used. In general, Lagrange's equation is given by

$$\frac{\mathrm{d}}{\mathrm{d}t}\left(\frac{\partial T}{\partial \dot{q}_i}\right) - \frac{\partial T}{\partial q_i} + \frac{\partial U}{\partial q_i} + \frac{\partial D}{\partial \dot{q}_i} = Q_i \tag{1}$$

where q_i, T, U, D, and Q_i are generalized coordinates, kinetic energy, potential energy, Rayleigh's dissipation function, and generalized forces, respectively. Equation (1) will be used directly for elastic motion. For rigid-body motion it is easier to express Lagrange's equations of motion in body-fixed frame of reference.

For structural modeling, it is assumed that the elastic deformation of the vehicle is sufficiently small and can be represented in terms of its normal undamped modes of free vibration. Hence, for a given

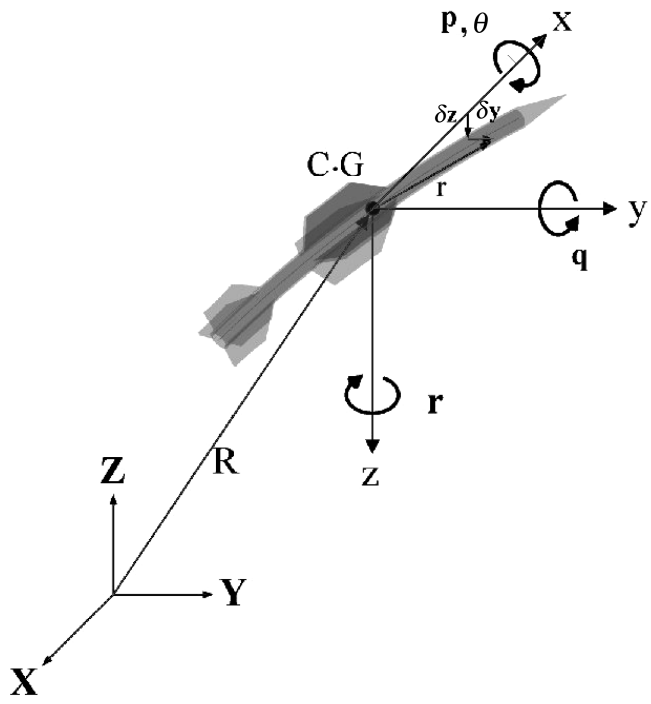

Fig. 1 Elastic flight vehicle with inertial and body frames of references.

mass element, the bending and torsional elastic deformations can be modeled as

$$\delta y = \sum \phi_i(x)\eta_i(t), \qquad \delta z = \sum \phi_i(x)\zeta_i(t)$$
$$\theta_x = \sum \theta_i(x)\gamma_i(t) \tag{2}$$

where ϕ_i and θ_i are the bending and torsional normal modes, respectively, and η_i, ζ_i, and γ_i are taken as the generalized coordinates. Finally, at a given mass element, the total elastic deformation can be modeled as

$$\boldsymbol{e} = \begin{Bmatrix} e_x \\ e_y \\ e_z \end{Bmatrix} = \begin{Bmatrix} 0 \\ \delta y - z\theta_x \\ \delta z + y\theta_x \end{Bmatrix} = \begin{Bmatrix} 0 \\ \sum_{i=1}^{\infty}(\phi_i\eta_i - z\theta_i\gamma_i) \\ \sum_{i=1}^{\infty}(\phi_i\zeta_i + y\theta_i\gamma_i) \end{Bmatrix} \tag{3}$$

Assuming constant mass and symmetry about the x-axis of the vehicle, using Coriolis' law and after some manipulation, the final expression for the kinetic energy of the vehicle is obtained:

$$\begin{aligned} T = {} & \frac{1}{2}m\boldsymbol{V}\cdot\boldsymbol{V} + \frac{1}{2}I(r^2+q^2) + \frac{1}{2}I_x p^2 \\ & + \frac{1}{2}\sum_{i=1}^{\infty} M_i\left[\dot{\eta}_i^2 + \dot{\zeta}_i^2 + p^2\left(\zeta_i^2 + \eta_i^2\right) + (q\zeta_i - r\eta_i)^2\right. \\ & \left. + 2p\left(\dot{\eta}_i\zeta_i - \dot{\zeta}_i\eta_i\right)\right] + \frac{1}{2}\left(p^2 + \frac{q^2+r^2}{2}\right)\sum_{i=1}^{\infty} J_i\gamma_i^2 \\ & + \frac{1}{2}\sum_{i=1}^{\infty} J_i\dot{\gamma}_i^2 \end{aligned} \tag{4}$$

where m is the mass of vehicle and $I_y = I_z = I$ is the mass moments of inertia about the y- (or z)-axis, I_x is the mass moment of inertia about the x-axis, and M_i and J_i are the generalized masses according to generalized coordinates η_i (or ζ_i) and γ_i, respectively.

In the present formulation the gravity is taken as an external force acting on the vehicle; thus, it is not a part of the potential energy. Therefore only the elastic strain energy is considered, which can be expressed in terms of the generalized coordinates η_i, ζ_i, and γ_i and modal natural frequencies ω_i and Ω_i, as follows:

$$U_e = \frac{1}{2}\sum_{i=1}^{\infty} M_i\omega_i^2\left(\eta_i^2 + \zeta_i^2\right) + \frac{1}{2}\sum_{i=1}^{\infty} J_i\Omega_i^2\gamma_i^2 \tag{5}$$

Also, Rayleigh's dissipation function in terms of the generalized coordinates can be written as

$$D = \frac{1}{2}\sum_{i=1}^{\infty} 2\mu_i\omega_i M_i\left(\dot{\eta}_i^2 + \dot{\zeta}_i^2\right) + \frac{1}{2}\sum_{i=1}^{\infty} 2\nu_i\Omega_i J_i\dot{\gamma}_i^2 \tag{6}$$

where μ_i and ν_i are the critical damping ratio of the ith bending and torsional mode, respectively.

Now equations of motion can be derived from Lagrange's equation [Eq. (1)] in terms of kinetic energy, potential energy and Rayleigh's dissipation function. The right-hand side of equations of motion are the generalized forces which can be represented using the principles of virtual work as follows,

$$Q_i = \frac{\partial(\delta W)}{\partial(\delta q_i)} \tag{7}$$

where δW is the virtual work done during a virtual displacement along the generalized coordinates, δq_i. The generalized aerodynamic forces can be evaluated in terms of the lift curve derivatives, L_β and L_α, and the local angles of attack and sideslip, $\alpha(x,t)$ and $\beta(x,t)$ [5]. Rigid-body angles of attack and sideslip for small angles are

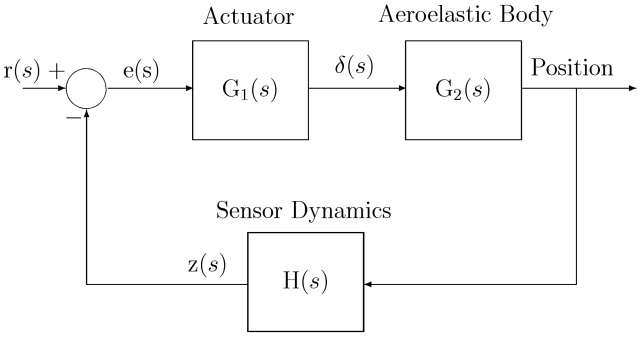

Fig. 2 Control loop.

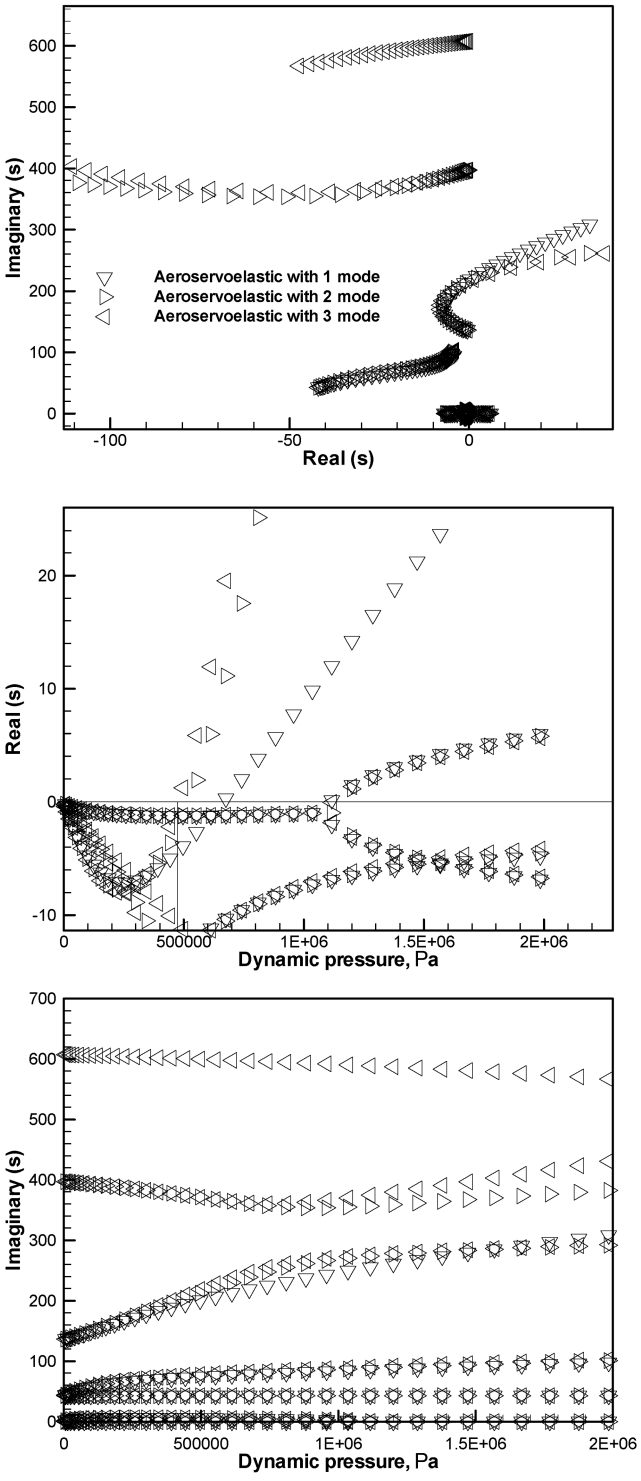

Fig. 3 Frequency and damping of the aeroservoelastic vehicle vs dynamic pressure for $k_A = 0.025$.

$$\alpha = \frac{w}{u}, \qquad \beta = \frac{v}{u} \tag{8}$$

The aerodynamic loads on any control surface produce generalized control forces. The generalized forces due to the rudder deflection δR at x_R and elevator deflection δE at x_E are determined as follows:

$$F_y^c = L_{y_{\delta R}}\delta R, \qquad F_z^c = -L_{z_{\delta E}}\delta E \tag{9}$$

Similarly the generated moments due to the aileron deflection δA at x_A, elevator deflection, and rudder deflection are

$$M_x^c = M_{l_{\delta A}}\delta A, \qquad M_y^c = M_{m_{\delta E}}\delta E, \qquad M_z^c = M_{n_{\delta R}}\delta R \tag{10}$$

The symmetric assumption of vehicle yields

$$L_{z_{\delta E}} = L_{y_{\delta R}} = L_\delta, \qquad M_{m_{\delta E}} = M_{n_{\delta R}} = M_\delta \tag{11}$$

Control System

The block diagram shown in Fig. 2 is a simplified flight vehicle control system which is used for all channels. This diagram models a linear time invariant system, that is, of course, an approximation to the real nonlinear time-varying systems. The linear approximation is used extensively in the design and analysis of flight vehicle control systems. In Fig. 2, $r(s)$ is the reference command signal, $e(s)$ is the error signal, $\delta(s)$ is the control (actuator displacement) signal, and $z(s)$ is the feedback signal. The transfer function $G_1(s)$ represents the servoactuators that drive the aerodynamic control surfaces. The feedback $H(s)$ represents the transfer function of the rate-gyros in each channels. The sensed rates for elastic vehicle in three channels are $p + \sum_{i=1}^{\infty}\dot{\gamma}_i\theta_i(x_r)$, $q - \sum_{i=1}^{\infty}\dot{\zeta}_i\phi_i'(x_r)$, and $r + \sum_{i=1}^{\infty}\dot{\eta}_i\phi_i'(x_r)$ instead of p, q, and r, where x_r is the position of rate-gyro in the rigid vehicle. The equations that correspond to the diagram in three channels are (overbars represent Laplace transforms)

$$\delta\bar{E} - G_{1q}(s)H_q(s)\left[\bar{q} - \sum_{i=1}^{\infty} s\bar{\zeta}_i\phi_i'(x_r)\right] = G_{1q}(s)\bar{e}_q(s) \tag{12}$$

$$\delta\bar{R} - G_{1r}(s)H_r(s)\left[\bar{r} + \sum_{i=1}^{\infty} s\bar{\eta}_i\phi_i'(x_r)\right] = G_{1r}(s)\bar{e}_r(s) \tag{13}$$

$$\delta\bar{A} - G_{1p}(s)H_p(s)\left[\bar{p} + \sum_{i=1}^{\infty} s\bar{\gamma}_i\theta_i(x_r)\right] = G_{1p}(s)\bar{e}_p(s) \tag{14}$$

Linearized Aeroservoelastic Model

The following assumptions are made in deriving the aeroservoelastic model. The vehicle longitudinal velocity is constant and the thrust, gravity, and drag forces are ignored. Assume p, q, r, v, w, ζ_i, η_i, and γ_i are small and retained only up to the first-order terms. Using these assumptions the roll channel decouples. Hence, the governing equations for the roll channel in Laplace domain can be written as

$$\begin{bmatrix} I_x s + M_p & -M_{l_{\delta A}} & 0 & \cdots \\ G_{1_p}(s)H_p(s) & 1 & sG_{1_p}(s)H_p(s)\theta_1(x_r) & \cdots \\ J^1 & -\frac{1}{J_1}M_{l\delta}^c\theta_1(x_A) & s^2 + 2v_i\Omega_i s + \Omega_i^2 + J^{11} & \cdots \\ \vdots & \vdots & \vdots & \ddots \end{bmatrix} \begin{Bmatrix} \bar{p} \\ \overline{\delta A} \\ \overline{\gamma_1} \\ \vdots \end{Bmatrix} = \begin{Bmatrix} 0 \\ G_{1p}(s)\overline{e}_p(s) \\ 0 \\ \vdots \end{Bmatrix} \tag{15}$$

where

$$M_p = \frac{1}{2u}\sum_{j=1}^{N_w} r_j L_{\alpha_j}, \qquad J^i = \frac{1}{2uJ_i}\sum_{j=1}^{N_w} L_{\alpha_j}\theta_i(x_j)r_j, \qquad J^{ik} = \frac{1}{2uJ_i}\sum_{j=1}^{N_w} L_{\alpha_j}\theta_i(x_j)\theta_k(x_j)r_j \tag{16}$$

Note that $L_{\alpha_j} = L_{\beta_j}$ and N_w is the total number of wing sets. For the pitch and yaw channels using the following definitions,

$$\xi = \beta + i\alpha, \qquad \Omega = q + ir, \qquad \delta_i(t) = \eta_i(t) + i\zeta_i(t), \qquad \delta C = \delta E + i\delta R \tag{17}$$

one can write the following system of equations

$$\begin{bmatrix} mus + L_\alpha & i\left(\frac{M_\alpha}{u} - mu\right) & iL_\delta & \frac{I_1^1 s}{u} - I_3^1 & \cdots \\ -M_\alpha & iIs + \frac{ic_q}{u} & iM_\delta & I_4^1 - \frac{I_2^1 s}{u} & \cdots \\ 0 & G_{1r}(s)H_r(s) & 1 & isG_{1r}(s)H_r(s)\phi_1'(x_r) & \cdots \\ I_1^1 & -\frac{iI_2^1}{u} & iL_\delta\phi_1(x_f) & \begin{matrix} M_1 s^2 + 2M_1\mu\omega s \\ +M_1\omega^2 - I_6^{11} + \frac{I_5^{11}s}{u} \end{matrix} & \cdots \\ \vdots & \vdots & \vdots & \vdots & \ddots \end{bmatrix} \begin{Bmatrix} \xi \\ \Omega \\ \overline{\delta C} \\ \overline{\delta_1} \\ \vdots \end{Bmatrix} = \begin{Bmatrix} 0 \\ 0 \\ G_{1r}(s)\overline{e}_r \\ 0 \\ \vdots \end{Bmatrix} \tag{18}$$

The required constants in Eq. (18) are tabulated in Table 1.

Table 1 Required constants

$L_\alpha = \int_L L_\alpha(x)\,dx$	$M_\alpha = \int_L xL_\alpha(x)\,dx$
$I_\alpha = \int_L x^2 L_\alpha(x)\,dx$	$M_i = \int_L \phi_i^2(x)m(x)\,dx$
$I_1^i = \int_L L_\alpha(x)\phi_i(x)\,dx$	$I_2^i = \int_L xL_\alpha(x)\phi_i(x)\,dx$
$I_3^i = \int_L L_\alpha(x)\phi_i'(x)\,dx$	$I_4^i = \int_L xL_\alpha(x)\phi_i'(x)\,dx$
$I_5^{ij} = \int_L L_\alpha(x)\phi_j(x)\phi_i(x)\,dx$	$I_6^{ij} = \int_L L_\alpha(x)\phi_i(x)\phi_j'(x)\,dx$

Table 2 Comparison of divergence results

Method	Divergence pressure, kPa
Engineering method ([10])	1149
Method of [5]	1089
Present work	1087

These relations are the aeroservoelastic equations of motion that correspond to the rigid-body translation and rotation as well as the elastic deformation and the control system of the vehicle. The governing system of equations must be solved simultaneously to determine the aeroservoelastic stability of the system.

Numerical Results

To demonstrate the validity of the proposed model, its application are presented for some test cases. First, the aeroelastic divergence of a specified configuration is determined. The required data for this example are presented in [10]. The results of static aeroelastic analysis of the test case, without the control loop, is tabulated in Table 2 where comparison with the other available research is also noted. The results show that using the first mode of vibration is sufficient for determination of this type of instability. The effect of control system dynamics is studied numerically in the next step by adding control loop to the previous test case. For this purpose the actuator and rate-gyro dynamic are assumed as

$$G_1(s) = \frac{k_A}{s(1+\tau_A s)}, \qquad H(s) = \frac{k_R s}{1 + 2(\zeta s/\omega_n) + s^2/\omega_n^2} \quad (19)$$

where τ_A, k_R, ζ, and ω_n are taken to be 0.002, 0.13, 0.7, and 60, respectively, and k_A is the gain of the control system. In the next step, for the gain value of $k_A = 0.025$, the eigenvalues are determined and shown in Fig. 3 for various values of dynamic pressure. It can be concluded that at least three mode shapes must be used for flutter determination. An important observation is that the combination of a stable aeroelastic and dynamic system may result in an unstable aeroservoelastic system. Finally the results of instability computations for various values of k_A are presented in Fig. 4. It can be seen whereas the flutter dynamic pressure is a function of the control system gain, divergence pressure and flutter frequency are independent of the control system gain variation. Because the first torsional frequency in most of the practical cases is several times larger than the first bending frequency, it can be concluded that no kind of instabilities may occur in this channel.

Conclusions

An analytical procedure for aeroservoelastic stability analysis of guided supersonic flight vehicles is developed using slender body aerodynamic theory and modal analysis techniques. It is shown that the roll channel is decoupled from pitch and yaw channels by using the linearized system of equations. Results indicate that divergence is the only aeroelastic instability that can occur for the nonrolling flight vehicle with no-control loop and is accurately computed using the first bending mode shape. The result of divergence analysis demonstrates that the vehicle elasticity has a destabilizing effect on the pitch and yaw channels. An important conclusion of this study

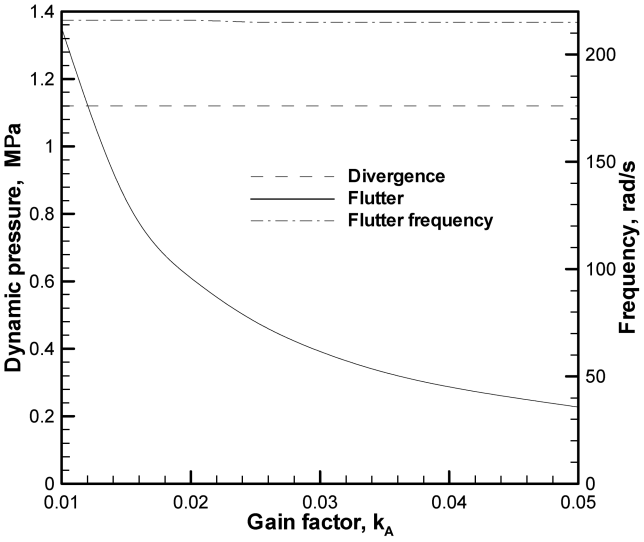

Fig. 4 Variation of aeroservoelastic instability parameters vs control system gain.

verifies that inclusion of aeroservoelasticity in the analysis can cause dynamic instability, even if the guided rigid vehicle is stable and the elastic vehicle is also stable in no-control loop flight. The indication is that the control loop can destabilize the bending motion of the vehicle. Fortunately this type of instability can be controlled by some parameter adjustments in the control system. In addition, it is observed that the control system gain variation does not affect the static divergence dynamic pressure and flutter frequency.

Acknowledgment

The author acknowledges Sharif University of Technology for financial support of this work (Grant 71/924).

References

[1] Meirovitch, L., and Nelson, H. D., "On the High-Spin Motion of a Satellite Containing Elastic Parts," *Journal of Spacecraft and Rockets*, Vol. 3, No. 11, 1966, pp. 1597–1602.

[2] Meirovitch, L., and Wesley, D. A., "On the Dynamic Characteristics of a Variable-Mass Slender Elastic Body Under High Accelerations," *AIAA Journal*, Vol. 5, No. 8, 1967, pp. 1439–1447.

[3] Oberholtzer, N. W., Schmidt, L. E., and Larmour, R. A., "Aeroelastic Behavior of Hypersonic Re-Entry Vehicles," AIAA Paper 83-0033, 1983.

[4] Crimi, P.,"Aeroelastic Stability and Response of Flexible Tactical Weapons," AIAA Paper 84-0392; 1984

[5] Platus, D. H.,"Aeroelastic Stability of Slender, Spinning Missiles," *Journal of Guidance, Control, and Dynamics*, Vol. 15, No. 1, 1992, pp. 144–151.

[6] Bilimoria, K. D., and Schmidt, D. K., "Integrated Development of the Equation of Motion for Elastic Hypersonic Flight Vehicles," *Journal of Guidance, Control, and Dynamics*, Vol. 18, No. 1, 1995, pp. 73–81.

[7] Newman, B., and Schmidt, D. K., "Numerical and Literal Aeroelastic-Vehicle-Model Reduction for Feedback Control Synthesis," *Journal of Guidance, Control, and Dynamics*, Vol. 14, No. 5, 1991, pp. 943–953.

[8] Livneh, R., and Schmidt, D. K., "Unified Literal Approximations for Longitudinal Dynamics of Flexible Vehicles," *Journal of Guidance, Control, and Dynamics*, Vol. 18, No. 5, 1995, pp. 1074–1083.

[9] Pourtakdoust, S. H., and Assadian, N., "Investigation of Thrust Effect on the Vibrational Characteristics of Flexible Guided Missiles," *Journal of Sound and Vibration* Vol. 272, Nos. 1–2, April 2004, pp. 287–299.

[10] Elyada, D., "Closed-Form Approach to Rocket-Vehicles Aeroelastic Divergence," *Journal of Spacecraft and Rockets*, Vol. 26, No. 2, 1989, pp. 95–102.